The interplay between mass, volume, θ, and $\langle\,\overline{\psi}\psi\,\rangle$ in N-flavor QED$_2$

J. E. Hetrick[1], Y. Hosotani[2], and S. Iso[3]
[1]*Department of Physics, University of Arizona, Tucson, Arizona 85721, USA*
[2]*School of Physics and Astronomy, University of Minnesota, Minneapolis, Minnesota 55455, USA*
[3]*Department of Physics, University of Tokyo, Tokyo 113, Japan*
(October 13, 1995)

The Schwinger model (QED$_2$) with N flavors of massive fermions on a circle of circumference L, or equivalently at finite temperature T, is reduced to a quantum mechanical system of $N-1$ degrees of freedom. With degenerate fermion masses (m) the chiral condensate develops a cusp singularity at $\theta = \pm\pi$ in the limit $L \to \infty$ or $T \to 0$,which is removed by a large asymmetry in the fermion masses. Physical quantities sensitively depend on the parameter mL or m/T, and the $m \to 0$ and $L \to \infty$ (or $T \to 0$) limits do not commute. A detailed analysis is given for $N = 3$.

PACS numbers: 11.10.Kk, 11.30.Hv, 12.38.Lg, 12.20.-m
Report numbers: AZPH-TH/95-25, UMN-TH-1410/95, UT-722
E-print: hep-th/9510090

Two-dimensional QED has profound resemblance to four-dimensional QCD, including chiral symmetry breaking, confinement, instantons, and θ vacua [1]. Defined on a circle [2–4], the model is mathematically equivalent to its finite temperature version [5], and recently the model with general fermion content was studied in connection with Z_n symmetry breaking [6]. A subtle difference between the massless and massive theories has been noted there, for which the non-commutativity of the massless limit and zero temperature limit is an crucial factor. In lattice gauge theory, the commutivity of the two limits $m \to 0$ and $L \to \infty$ is subtle and important. This is particularly true in the issue of the triviality of QED$_4$ at strong coupling [7].

In a previous paper [8] we have shown that massive two-flavor QED$_2$ defined on a circle is reduced to the quantum mechanics of a pendulum. The physics is controlled by the strength of the pendulum potential κ, which is given in a large volume L by $\kappa \sim mL(eL)^{1/2}|\cos\frac{1}{2}\theta|$ where e, m, and θ are the coupling constant, fermion mass, and vacuum angle, respectively. It was recognized that $L \to \infty$ and $m \to 0$ limits do not commute. Here we generalize our analysis to the N-flavor case.

The $N \geq 2$ Schwinger model is distinctively different from the $N = 1$ model. With massless fermions the spectrum contains $N-1$ massless bosons (mesons), and the chiral condensate vanishes, $\langle\,\overline{\psi}\psi\,\rangle = 0$. [9] With massive fermions, the boson masses and chiral condensate are non-vanishing, but have singular dependence on m and θ at $\theta = \pm\pi$ in the $L \to \infty$ limit. [10]

Suppose that the fermion and gauge fields obey anti-periodic and periodic boundary conditions, respectively. The model, after a Wick rotation, is equivalent to the model on a line at finite temperature $T = L^{-1}$.

In the bosonization method

$$\psi^a_\pm = \frac{C^a_\pm}{\sqrt{L}}\, e^{\pm i\{q^a_\pm + 2\pi p^a_\pm (t\pm x)/L\}} : e^{\pm i\sqrt{4\pi}\phi^a_\pm(t,x)} : \tag{1}$$

where $C^a_\pm$ is the Klein factor. We refer the reader to [8] for details. Anti-Periodicity for the fermions is ensured by a physical state condition $e^{2\pi i p^a_\pm}\,|\,\text{phys}\,\rangle = |\,\text{phys}\,\rangle$. Thus $p^a_\pm$ takes integer values.

The Hamiltonian in the Schrödinger picture becomes

$$\begin{aligned}
H_{\rm tot} &= H_0 + H_{\rm osci} + H_{\rm mass} + (\text{constant}) \\
H_0 &= -\frac{e^2L}{2}\frac{d^2}{d\Theta_W^2} + \frac{N}{2\pi L}\Big\{\Theta_W + \frac{\pi}{N}\sum_{a=1}^N (p^a_+ + p^a_-)\Big\}^2 - \frac{\pi}{2NL}\Big\{\sum_{a=1}^N (p^a_+ + p^a_-)\Big\}^2 + \frac{\pi}{L}\sum_{a=1}^N \Big\{(p^a_+)^2 + (p^a_-)^2\Big\} \\
H_{\rm osci} &= \int dx\, \frac{1}{2}\Big[\sum_{a=1}^N \Big\{\,\Pi_a^2 + (\phi_a')^2\Big\} + \frac{e^2}{\pi}\Big(\sum_{a=1}^N \phi_a\Big)^2\Big].
\end{aligned} \tag{2}$$

Θ_W is the Wilson line phase around the circle: $A_1 = \Theta_W(t)/eL$. It couples to $p^a_\pm$'s through the chiral anomaly [3]. $\phi_a = \phi^a_+ + \phi^a_-$ and Π_a is its canonical conjugate.

In the absence of fermion masses the Hamiltonian is exactly solvable. The spectrum contains one massive field $N^{-1/2}\sum_{a=1}^{N}\phi_a$ with a mass $\mu=(N/\pi)^{1/2}e$, and $N-1$ massless fields. The mass term $H_{\rm mass}=\int_0^L dx\sum_a m_a\overline{\psi}_a\psi_a$ however gives various interactions among the zero and ϕ modes. We present an algorithm valid for $|m_a|\ll e$ to evaluate the effects of $H_{\rm mass}$. We stress that this by no means implies that $H_{\rm mass}$ can be treated as a small perturbation. On the contrary, it dominates over H_0 in the $L\to\infty$ or $T\to 0$ limit; its effects are quite non-perturbative.

As $H_{\rm mass}$ commutes with $p_+^a-p_-^a$, we restrict ourselves to states with $(p_+^a-p_-^a)\,|\,{\rm phys}\,\rangle=0$. Then a complete set of eigenfunctions of H_0 is $\Phi_s^{(n_1,\cdots,n_N)}\sim u_s\big[\Theta_W+(2\pi\sum_a n_a/N)\big]\,e^{i\sum n_a(q_+^a+q_-^a)}$ where u_s satisfies $\frac{1}{2}(-\partial_x^2+x^2)u_s=(s+\frac{1}{2})u_s$ with $\Theta_W=(\pi e^2L^2/N)^{1/4}x$. The ground states of H_0 are infinitely degenerate for $n_1=\cdots=n_N$.

It proves to be much more convenient to work in a coherent state basis $\Phi_s(\varphi_1,\cdots,\varphi_{N-1};\theta)$ given by

$$\Phi_s(\varphi_a;\theta)\sim\sum_{\{n,r_a\}}e^{in\theta+i\sum r_a\varphi_a}\;\Phi_s^{(n+r_1,\cdots,n+r_{N-1},n)}\tag{3}$$

$H_{\rm tot}$ induces transitions among $\Phi_s(\varphi_a;\theta)$. However the effect of transitions in the s index is small [8] and we restrict ourselves to $s=0$ states. The vacuum state is written as

$$\Phi_{\rm vac}(\theta)=\int_0^{2\pi}d\varphi_1\cdots d\varphi_{N-1}\;f(\varphi_a;\theta)\;\Phi_0(\varphi_a;\theta)\ .\tag{4}$$

$H_{\rm mass}$ significantly alters the vacuum structure of the ϕ_a modes as well. Its main effect is that the $N-1$ previously massless fields now acquire finite masses. The vacuum is defined with respect to these physical fields.

We write mass eigenstate fields as $\chi_\alpha=U_{\alpha a}\phi_a$. In this physical space $(p_+^a-p_-^a)\,|\,{\rm phys}\,\rangle=0$, the fermion mass operator $M_a=\overline{\psi}_a\frac{1}{2}(1+\gamma^5)\psi_a$ is (in the Schrödinger picture)

$$\begin{aligned}M_a&=-\frac{e^{i(q_-^a+q_+^a)}}{L}\prod_{\alpha=1}^{N}B(\mu_\alpha L)^{(U_{\alpha a})^2}N_{\mu_\alpha}[e^{iU_{\alpha a}\sqrt{4\pi}\chi_\alpha}]\\ B(z)&=\frac{z}{4\pi}\exp\left\{\gamma+\frac{\pi}{z}-2\int_1^\infty\frac{du}{(e^{uz}-1)\sqrt{u^2-1}}\right\}.\end{aligned}\tag{5}$$

Here $N_\mu[\cdots]$ indicates normal-ordering with reference to a mass μ. We have made use of $N_0[e^{i\beta\chi}]=B(\mu L)^{\beta^2/4\pi}N_\mu[e^{i\beta\chi}]$. [3] It is easy to find

$$\begin{aligned}\langle\,\Phi_s(\theta';\varphi_a')|H_{\rm mass}|\Phi_s(\theta;\varphi_a)\,\rangle&=-\delta_{2\pi}(\theta'-\theta)\prod_{b=1}^{N-1}\delta_{2\pi}(\varphi_b'-\varphi_b)\sum_{a=1}^{N}2m_aA_a\cos\varphi_a\\ A_a&=e^{-\pi/N\mu L}\prod_{\alpha=1}^{N}B(\mu_\alpha L)^{(U_{\alpha a})^2}\quad,\end{aligned}\tag{6}$$

where $\varphi_N=\theta-\sum_{a=1}^{N-1}\varphi_a$.

The equation $H_{\rm tot}\,\Phi_{\rm vac}(\theta)=E\,\Phi_{\rm vac}(\theta)$ becomes: $\Big\{-\triangle_N^\varphi+V_N(\varphi)\Big\}\;f(\varphi)=\dfrac{NEL}{2\pi(N-1)}\;f(\varphi)$, where

$$\begin{aligned}\triangle_N^\varphi&=\sum_{a=1}^{N-1}\frac{\partial^2}{\partial\varphi_a^2}-\frac{2}{N-1}\sum_{a<b}^{N-1}\frac{\partial^2}{\partial\varphi_a\partial\varphi_b}\\ V_N(\varphi)&=-\frac{NL}{(N-1)\pi}\;\sum_{a=1}^{N}m_aA_a\cos\varphi_a\quad.\end{aligned}\tag{7}$$

The potential $V_N(\varphi)$ depends, through A_α defined in (6), on μ_α and $U_{\alpha a}$ which are to be self-consistently determined from the wave function $f(\varphi_a;\theta)$. In the θ-vacuum (4), $\langle\,M_a\,\rangle_\theta=-(A_a/L)\,\langle\,e^{-i\varphi_a}\,\rangle_f$ where the f-average is defined by $\langle\,g(\varphi)\,\rangle_f=\int[d\varphi]\,g(\varphi)|f(\varphi)|^2$.

$V_N(\varphi)$ has a similar structure to the potential which appears in the effective chiral Lagrangian of QCD. In Witten's formalism [11] the φ_a's are related to the pseudoscalar mesons themselves. The constraint $\sum_{a=1}^{N}\varphi_a=\theta$ appears when the chiral anomaly dominates over the quark masses. In our case the χ_α's represent the boson fields, whereas φ_a's are

parameters of the coherent state basis. The similar structure emerges as a result of the pattern of $SU(N)\times SU(N)$ symmetry breaking.

To find the boson masses μ_α, we denote

$$\begin{pmatrix} R_a \\ I_a \end{pmatrix} = \frac{8\pi}{L}\, m_a A_a \cdot \begin{pmatrix} Re \\ Im \end{pmatrix} \langle\, e^{-i\varphi_a}\,\rangle_f ~. \tag{8}$$

$H_{\rm mass}$ yields $\prod_\alpha N_{\mu_\alpha}[e^{iU_{\alpha a}\sqrt{4\pi}\chi_\alpha}]$. Expanding χ_α in $H_{\rm mass}$ and adding the contribution from the chiral anomaly, one finds

$$H^\chi_{\rm mass} = \int dx\, \left\{ \frac{U_{\alpha a} I_a}{\sqrt{4\pi}}\, \chi_\alpha + \frac{1}{2}\,\mu_\alpha^2\,\chi_\alpha^2 + {\rm O}(\chi^3) \right\} ~. \tag{9}$$

Here $U_{\alpha a}$ diagonalizes the matrix

$$\frac{\mu^2}{N}\begin{pmatrix} 1 & \cdots & 1 \\ \vdots & \ddots & \vdots \\ 1 & \cdots & 1 \end{pmatrix} + \begin{pmatrix} R_1 & & \\ & \ddots & \\ & & R_N \end{pmatrix} ~~, \tag{10}$$

and μ_α are the eigenvalues. (6), (7), (8), and the diagonalization of (10) must be solved simultaneously.

Suppose that all fermion masses are degenerate: $m_a = m \ll e$. In this case $R_a = R$ and $\langle\, e^{-i\varphi_a}\,\rangle_f = \langle\, e^{-i\varphi}\,\rangle_f$. One can choose $U_{\alpha a}$ such that $U_{1a}=N^{-1/2}$, $\mu_1^2 = \mu^2 + R$, and $\mu_2^2 = \cdots = \mu_N^2 = R$. The potential and boson masses are reduced to

$$\begin{aligned}
V_N(\varphi) = &~ - \kappa_0 \sum_{a=1}^N \cos\varphi_a \\
\kappa_0 = &~ \frac{NmL}{(N-1)\pi}~ B(\mu_1 L)^{\frac{1}{N}} B(\mu_2 L)^{1-\frac{1}{N}}~ e^{-\pi/N\mu L} \\
\frac{\mu_2^2}{4\pi} = &~ \frac{2\pi}{L^2}\,\frac{N-1}{N}\,\kappa_0 \,\langle\, \cos\varphi\,\rangle_f = -m\,\langle\, \bar\psi_a \psi_a\,\rangle_\theta ~~.
\end{aligned} \tag{11}$$

The last relation is analogous to the PCAC relation in QCD [12]. The strength κ_0 and θ fix the potential $V_N(\varphi)$, and thus control the physical behavior. Since $B(z)\sim e^\gamma z/4\pi$ for $z\gg 1$ and $B(0)=1$, $\kappa_0\to\infty$ (0) as $L\to\infty$ (0). So long as $m\neq 0$, the location of the minimum of the potential determines the physics at $L\to\infty$.

The potential $V_N(\varphi)$ has a minimum at

$$\varphi_1 = \cdots = \varphi_N = \frac{1}{N}\Big(\theta - 2\pi\Big[\frac{\theta+\pi}{2\pi}\Big]\Big) \equiv \frac{1}{N}\,\bar\theta(\theta) \tag{12}$$

$[-\pi\le\bar\theta<\pi]$; its location jumps discontinuously at $\theta=\pi$ from $\varphi_a=\pi/N$ to $\varphi_a=-\pi/N$. There is a special feature in the $N=2$ case: as $V_2(\varphi) = -2\kappa_0\cos\frac{1}{2}\theta\cos(\varphi_1-\frac{1}{2}\theta)$, the potential vanishes at $\theta=\pm\pi$. Its behavior is controlled by the single parameter $\kappa_0|\cos\frac{1}{2}\theta|$ (see [8]).

When $\kappa_0\gg 1$ (or as $L\to\infty$), the wave function $f(\varphi)$ approaches a delta function around the minimum of the potential $V_N(\varphi)$. Hence $\lim_{L\to\infty}\langle\, \cos\varphi_a\,\rangle_f = \cos(\bar\theta/N)$. For $m/\mu\ll 1$ one finds from (11)

$$\frac{1}{\mu}\,\langle\, \bar\psi\psi\,\rangle_\theta = -\frac{1}{4\pi}\Big(2e^\gamma\cos\frac{\bar\theta}{N}\Big)^{\frac{2N}{N+1}}\Big(\frac{m}{\mu}\Big)^{\frac{N-1}{N+1}} ~. \tag{13}$$

In the opposite limit $\kappa_0\ll 1$, the wave function is given by $f=(2\pi)^{-(N-1)/2}\big\{1+\kappa_0\sum_{a=1}^N\cos\varphi_a+\cdots\big\}$ so that

$$\langle\, \cos\varphi_a\,\rangle_f = \begin{cases} (1+\cos\theta)\kappa_0 & \text{for } N=2 \\ \kappa_0 & \text{for } N\ge 3. \end{cases} \tag{14}$$

For $N\ge 3$ and $\mu L\ll 1$,

$$\frac{1}{\mu}\,\langle\, \bar\psi\psi\,\rangle_\theta = -\frac{2N}{\pi(N-1)}\,\frac{m}{\mu}\,e^{-2\pi/N\mu L}. \tag{15}$$

In the intermediate region, $\mu L \gg 1 \gg \mu_2 L$,

$$\frac{1}{\mu} \langle \overline{\psi}\psi \rangle_\theta = -\frac{2N}{\pi(N-1)} \frac{m}{\mu} \left(\frac{\mu L}{4\pi} e^\gamma\right)^{2/N} . \tag{16}$$

For $N = 2$, (15) and (16) must be multiplied by a factor $2\cos^2 \frac{1}{2}\theta$.

For general values of μL and m/μ, we have determined μ_2 and $\langle \overline{\psi}\psi \rangle_\theta$ in the $N = 3$ case numerically. Fig. 1 shows typical wave functions $|f(\varphi)|^2$ at $\kappa_0 = 0.1, 10$ and $\theta = 0,\ 0.999\pi$. In fig. 2, $\langle \overline{\psi}\psi \rangle/\mu$ at $\theta = 0$ and $\mu L = 10^3$ is plotted as a function of m/μ. In fig. 3, $\langle \overline{\psi}\psi \rangle/\mu$ at $\theta = 0$ is plotted as a function of T/μ and m/μ. In fig. 4, the θ dependence of $\langle \overline{\psi}\psi \rangle/\mu$ at $m/\mu = 10^{-3}$ is depicted for various μL.

Several important observations follow. As is evident from (13), $\langle \overline{\psi}\psi \rangle$ in the infinite volume limit has fractional power dependence on the fermion mass m. However, if the massless limit $m \to 0$ is taken with a finite L, then κ_0 becomes very small ($\kappa_0 \ll 1$) and $\langle \overline{\psi}\psi \rangle$ is given by either (15) or (16), which is linear in m. In this limit the fermion mass term in the Hamiltonian can be treated as a small perturbation. On the other hand, the effect of finite fermion masses in infinite volume is always non-perturbative. The massless and infinite volume limits do not commute with each other. The important parameter is κ_0. We have juxtaposed a plot for κ_0 in fig. 2 from which one can see that the crossover in physical behavior takes place around $\kappa_0 = 0.2$.

Our result can be reinterpreted for the Schwinger model on a line at finite temperature by replacing L by T^{-1}. We see that there is no phase transition at finite temperature. [5] The condensate $\langle \overline{\psi}\psi \rangle$, which is non-vanishing at $T = 0$, smoothly goes to zero at finite temperature. See fig. 3.

Thirdly all physical quantities are periodic in θ with period 2π. At $L = \infty$, $\langle \overline{\psi}\psi \rangle_\theta$ has a cusp at $\theta = \pm\pi$, [10] while at any finite L the cusp disappears as shown in fig. 4. The appearance of the cusp is traced back to the discontinuous jump in the location of the minimum of the potential $V_N(\varphi)$.

So far we have concentrated on cases with a symmetric fermion mass term. For a general fermion masses, the evaluation procedure is more involved. One important conclusion can be drawn. In the potential $V_N(\varphi)$ in (7), the coefficients of $\cos\varphi_a$ are all different in general. The potential for $N = 3$ is proportional to

$$F(\varphi) = -q\cos\varphi_1 - r\cos\varphi_2 - \cos(\theta - \varphi_1 - \varphi_2) \tag{17}$$

where $q = m_1A_1/m_3A_3$ and $r = m_2A_2/m_3A_3$. We have investigated the location of the minimum of $F(\varphi)$ as a function of θ with various parameter values (q, r). In the symmetric case $(q, r) = (1, 1)$, the location of the minimum moves from $(\varphi_1, \varphi_2) = (-\frac{1}{3}\pi, -\frac{1}{3}\pi)$ to $(\frac{1}{3}\pi, \frac{1}{3}\pi)$ as θ varies from $-\pi$ to $+\pi$, and jumps to return to the original point $(-\frac{1}{3}\pi, -\frac{1}{3}\pi)$; see fig. 5. Now we add an asymmetry. Several cases are plotted in fig. 5. One can see that so long as the asymmetry is small enough, there is a discontinuous jump at $\theta = \pm\pi$. However, a sufficiently large mass asymmetry removes this discontinuity. For instance, for $(q, r) = (1, 0.3)$, the minimum moves from $(\varphi_1, \varphi_2) = (0, -\pi)$ to $(0, +\pi)$, hence making a closed loop in the φ_1–φ_2 plane. We have observed that with sufficiently large asymmetry, the minimum at $\theta = \pm\pi$ is located at either $(0, 0)$, $(0, \pm\pi)$ or $(\pm\pi, 0)$. These three points are related by S_3 transformations.

We conclude that a sufficiently large asymmetry in the fermion masses removes the cusp singularity at $\theta = \pm\pi$ in $\langle \overline{\psi}\psi \rangle$ in the $L \to \infty$ limit. A similar conclusion has been drawn in the QCD context by Creutz. [13]

Acknowledgments

This work was supported in part by by the U.S. Department of Energy under contracts DE-FG03-95ER-40906 (J.H.) and by DE-AC02-83ER-40105 (Y.H.). J.H. would like to thank the ITP at U.C. Santa Barbara and the TPI at U. Minnesota, and Y.H. would like to thank the Aspen Center for Physics, for their hospitality where a part of this work was carried out.

---

[1] J. Schwinger, *Phys. Rev.* **125** 397 (1962); **128** 2425 (1962); J.H. Lowenstein and J.A. Swieca, *Ann. Phys. (N.Y.)* **68** 172 (1971). A. Casher, J. Kogut and L. Susskind, *Phys. Rev.* **D10** 732 (1974). S. Coleman, R. Jackiw, and L. Susskind, *Ann. Phys. (N.Y.)* **93** 267 (1975).

[2] N. Manton, *Ann. Phys. (N.Y.)* **159** 220 (1985);

[3] J.E. Hetrick and Y. Hosotani, *Phys. Rev.* **D38** 2621 (1988);
[4] R. Link, *Phys. Rev.* **D42** 2103 (1990). S. Iso and H. Murayama, *Prog. Theoret. Phys.* **84**142 (1990) .
[5] I. Sachs and A. Wipf, *Helv. Phys. Acta.* **65** 652 (1992).
[6] T.H. Hansson, H.B. Nielsen and I. Zahed, USITP-94-09, `hep-ph/9405324`
[7] M. Göckeler et al, *Nucl. Phys.* **B371** 713 (1992); A. Kocić, J.B. Kogut and M.-P. Lombardo, *Nucl. Phys.* **B398** 376 (1993); V. Azcoiti et al. `hep-lat/9509037`.
[8] J.E. Hetrick, Y. Hosotani and S. Iso, *Phys. Lett.* **B350** 92 (1995).
[9] M.B. Halpern, *Phys. Rev.* **D13** 337 (1976); I. Affleck, *Nucl. Phys.* **B265** [FS15] 448 (1986). C. Gattringer and E. Seiler, *Ann. Phys. (N.Y.)* **233** 97 (1994). H. Joos and S.I. Azakov, *Helv. Phys. Acta.* **67** 723 (1994). M.A. Shifman and A.V. Smilga, *Phys. Rev.* **D50** 7659 (1994).
[10] S. Coleman, *Ann. Phys. (N.Y.)* **101** 239 (1976).
[11] E. Witten, *Ann. Phys. (N.Y.)* **128** 363 (1980).
[12] A.V. Smilga, *Phys. Lett.* **B278** 371 (1992).
[13] M. Creutz, BNL-61796, `hep-th/9505112`.

Figures:

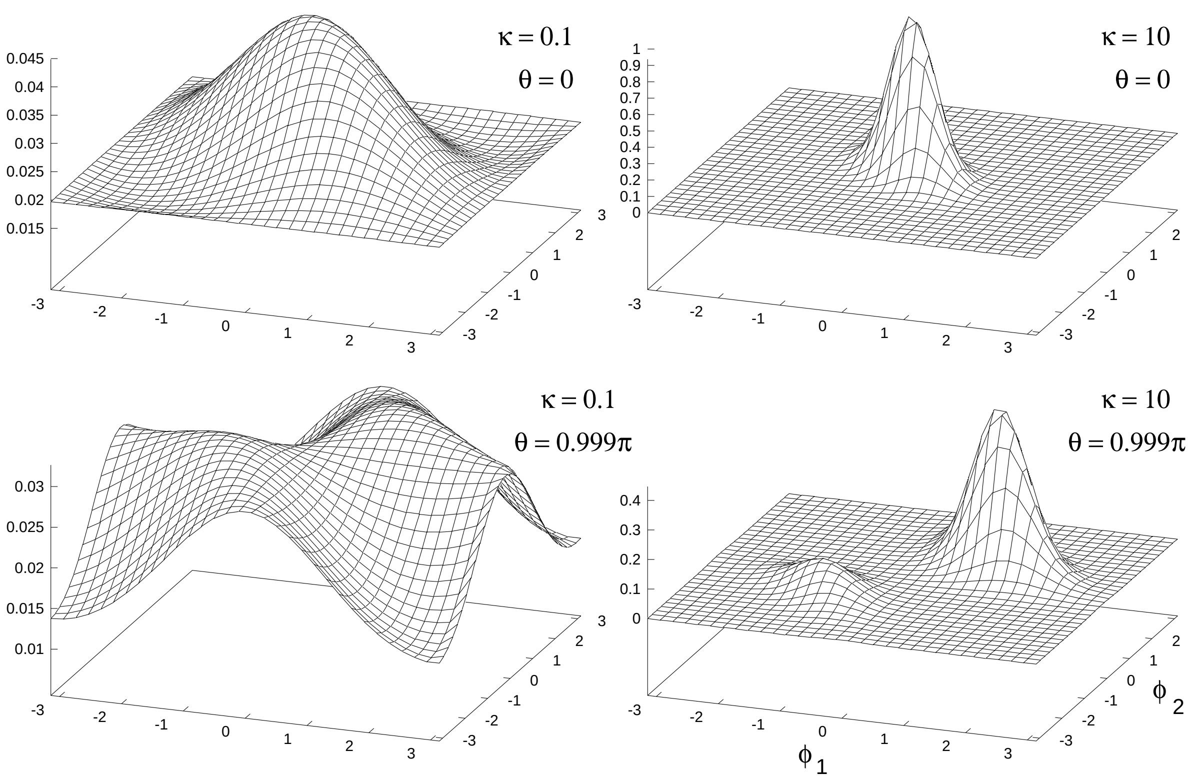

FIG. 1. Typical wave functions $|f(\varphi)|^2$ at $\kappa_0 = 0.1$ and 10, and $\theta = 0$ and 0.999π

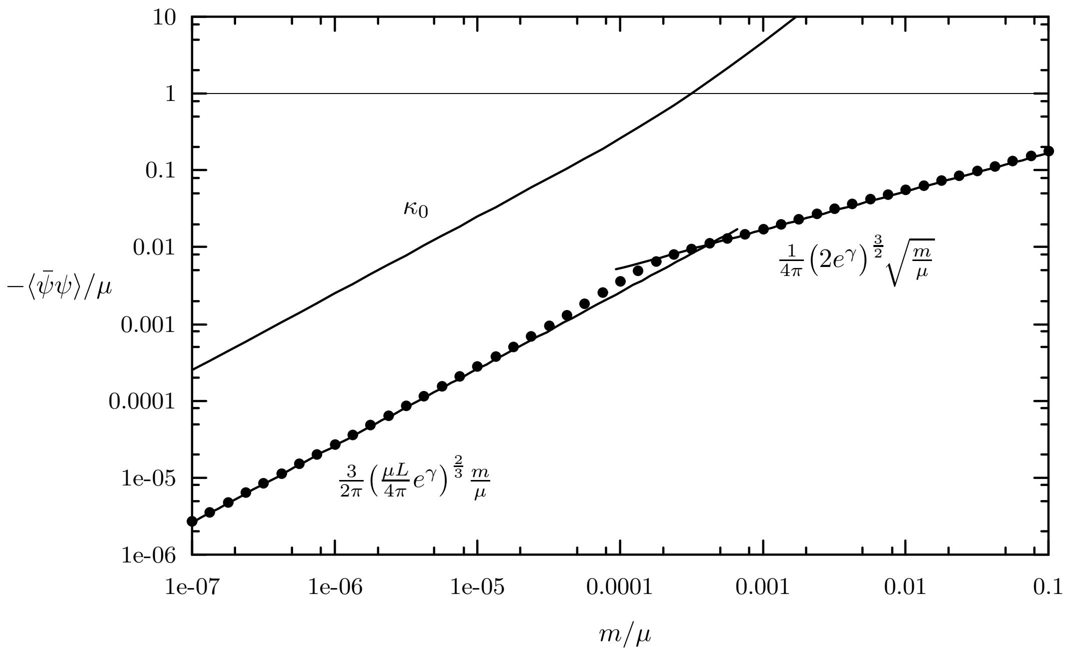

FIG. 2. The behavior of $= -\langle\,\overline{\psi}\,\psi\,\rangle/\mu$ versus m/μ at $\mu L = 10^3$ and $\theta = 0$. The analytic forms, (13) and (16), are also displayed. The crossover occurs at $\kappa_0 \approx 0.2$.

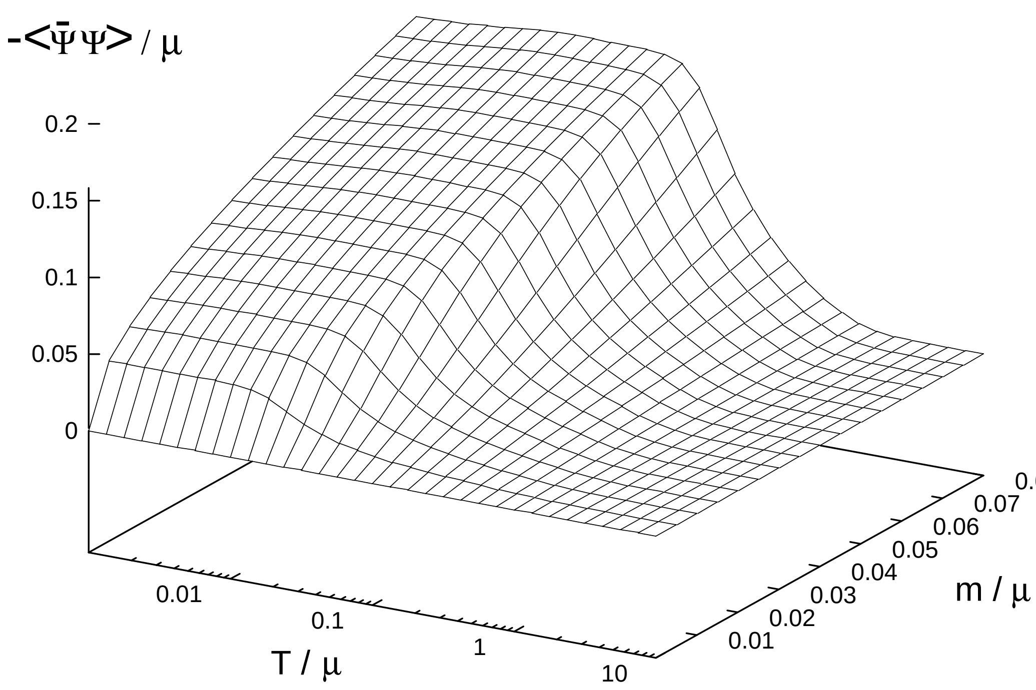

FIG. 3. The chiral condensate $\langle\,\overline{\psi}\,\psi\,\rangle/\mu$ as a function of temperature T/μ (or $1/\mu L$) at $\theta = 0$.

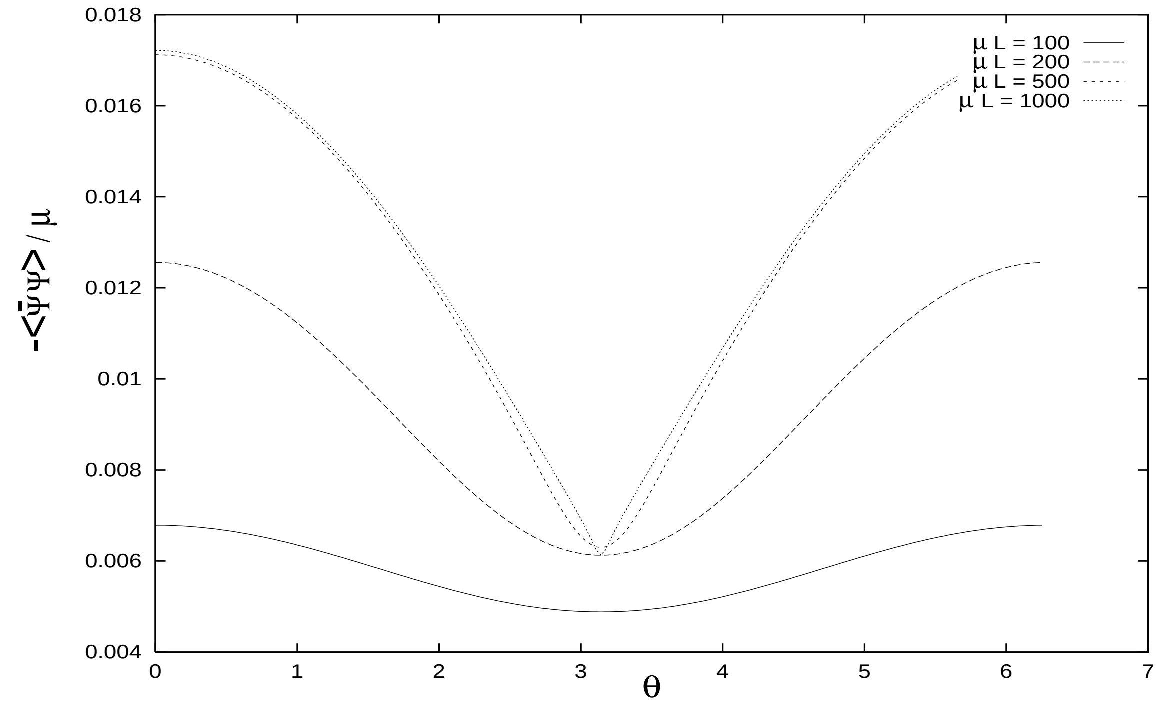

FIG. 4. The θ dependence of $\langle \bar{\psi}\psi \rangle$. In each case $m/\mu = 0.001$.

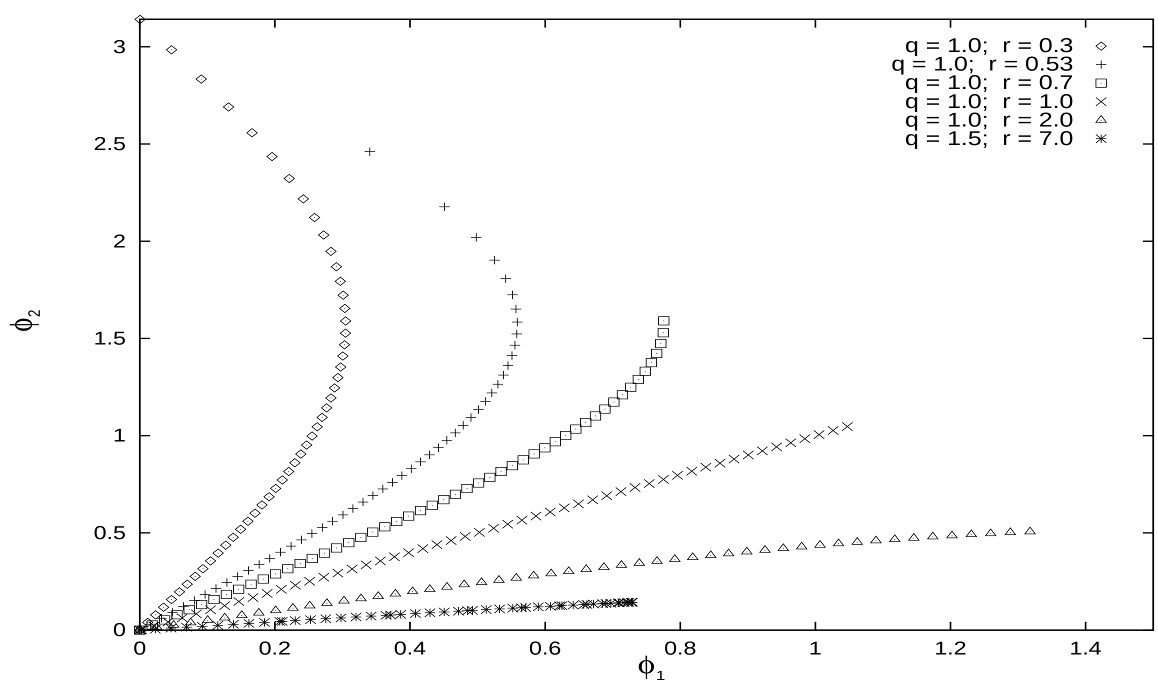

FIG. 5. The location of the minimum of $F(\varphi_1, \varphi_2)$ in (17). The points in the graph for each q and r pair run from $\theta = 0$ (at the origin) and end at $\theta = \pi$. For $\theta < 0$, the minimum is located at $(\varphi_1, \varphi_2)_\theta = -(\varphi_1, \varphi_2)_{-\theta}$. For $(q, r) = (1.5, 7)$ the minimum returns to the origin at $\theta = \pi$.